Adsorptive Desulfurization of Bioethanol-Derived Propylene Using Porous Iron Oxide

Takuji Yamamoto*, Akira Endo, Takao Ohmori

Research Institute for Innovation in Sustainable Chemistry, National Institute of Advanced Industrial Science and Technology (AIST), Central 5, 1-1-1 Higashi, Tsukuba, Ibaraki, 305-8565, Japan
yamamoto-t@aist.go.jp

In the development of the ethanol-to-olefin (ETO) conversion process to produce polymer-grade propylene from cellulosic bioethanol which contained an organosulfur impurity, adsorptive desulfurization of propylene using porous iron oxide (PIO) was examined. We evaluated the performance of PIO for the adsorption of hydrogen sulfide (HS), which was changed from the organosulfur impurity in bioethanol during the ETO conversion, by the measurement of a packed-bed breakthrough curve in a gas phase under the different temperature and pressure. We confirmed that PIO was capable of removing HS selectively from the mixed gas containing propylene, because of the reactivity of PIO with HS even at low temperature. The amount of adsorbed HS on PIO was found to increase with the increase in the temperature or pressure. As a result, the concentration of HS in the desulfurized gas could be reduced lower than 10 ppb.

1. Introduction

Because of the progress of global warming as well as the depletion of fossil fuel, cellulosic biomass has been expected as an alternative feedstock of bioethanol (Kravanja and Friedl, 2010; Porzio et al., 2011). Recently, synthesis of propylene by the ethanol to olefin (ETO) conversion is gaining an increasing interest from both scientific and engineering points of view (Song et al., 2009; Inoue et al., 2010; Goto et al., 2010; Furumoto et al., 2011) (Figure 1(a)). We have been developing a cost competitive process to produce polymer-grade propylene from cellulosic bioethanol.

As a result of analyzing various types of cellulosic bioethanol produced from different raw materials, we have confirmed that bioethanol contains organosulfur impurities, for example, dimethylsulfide (DMS), dimethylsulfoxide (DMSO) and dimethyldisulfide (DMDS) as shown in Figure 1(b). Although the detail of mechanism is still unknown, it is assumed that such sulfur impurities are derived from the raw material of bioethanol, the microorganisms used in the ethanol fermentation process (Landaud et al., 2008). We have also confirmed that it is difficult to remove the organosulfur impurities from ethanol efficiently (Chaichanawong et al., 2010). The organosulfur impurities contained in bioethanol are mostly converted to HS during the ETO conversion. It is requested that the concentration of HS in the polymer-grade propylene is lower than several tens of ppb to avoid poisoning of the catalyst used for the polymerization of propylene (Muroi, 2003). However, it is difficult to totally remove HS from propylene by the conventional distillation, since the boiling point of HS is close to that of propylene as summarized in Table 1. As a result, it is concerned that HS causes deactivation of the catalyst used for the polymerization of propylene.

Porous iron oxide (PIO) is one of the most effective and inexpensive adsorbents for the removal of HS. In the desulfurization processes of petroleum industry, PIO is usually used at the temperature higher
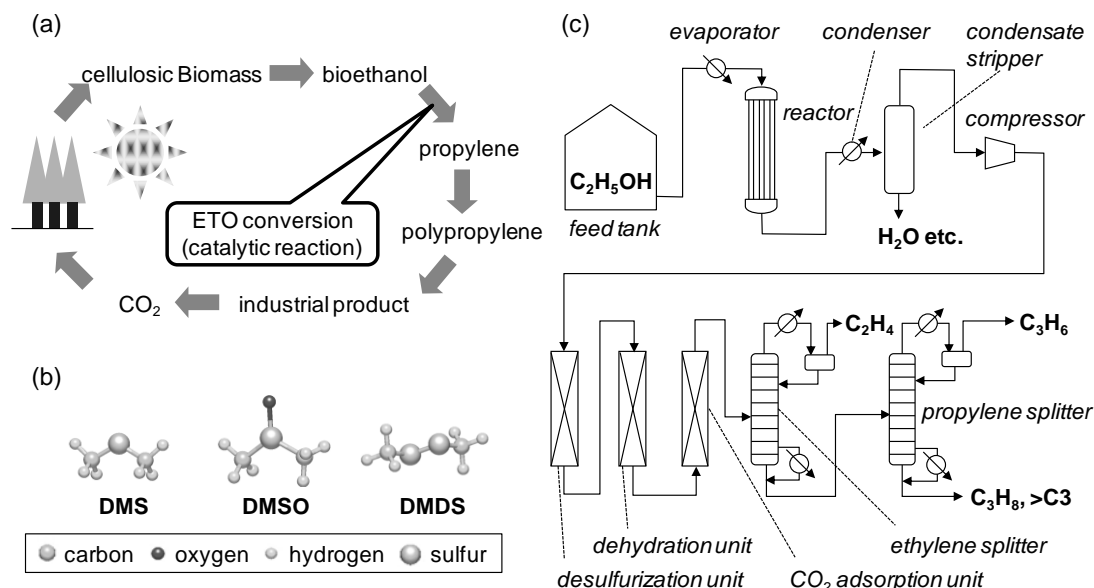
Figure 1: (a) Carbon cycle in the production of propylene from cellulosic biomass, (b) sulphur impurities contained in crude bioethanol, (c) schematic diagram of the process for the production of propylene by the ETO conversion.

Table 1: Comparison of boiling point of the compounds

compound	hydrocarbon			sulfur compounds			
	ethylene	propylene	propane	HS	DMS	DMDS	DMSO
boiling point [K]	170	226	231	213	308	383	462

than 800 K. On the other hand, as far as the authors have investigated, the adsorption mechanism of HS on PIO at relatively low temperature (< 400 K) has not yet been clarified. In this study, we examine the adsorptive removal of HS employing PIO in the process for producing polymer-grade propylene from cellulosic bioethanol as depicted in Figure 1(c). Then, we evaluate the effects of the temperature and pressure on the adsorption performance of PIO by the measurement of a packed-bed breakthrough curve (BTC).

2. Experimental

2.1 Material
PIO used in this study was supplied from the Japan Limonite Co., Ltd. PIO (limonite) was produced from natural soil containing approximately 70 wt.% of iron oxide, 14 wt.% of silica and 3 wt.% of alumina. Iron oxide contained in limonite was mostly goethite with the chemical formula of $FeO(OH) \cdot nH_2O$.

2.2 Characterization
The porous structure of PIO was determined by the adsorption measurement of N_2 at 77 K after outgassing at 473 K under vacuum for 2 h. The Brunauer–Emmett–Teller specific surface area of the sample was evaluated based on the adsorption isotherm. Pore size distribution of the sample was also determined by applying the Dollimore-Heal method to the desorption isotherm.
The performance of PIO for the adsorption of HS was evaluated by the measurement of a BTC using the apparatus as depicted in Figure 2 (a). The pellet of PIO was crushed and the particles with the grain size of 150-250 µm were employed in the measurement of a BTC. The PIO particles were
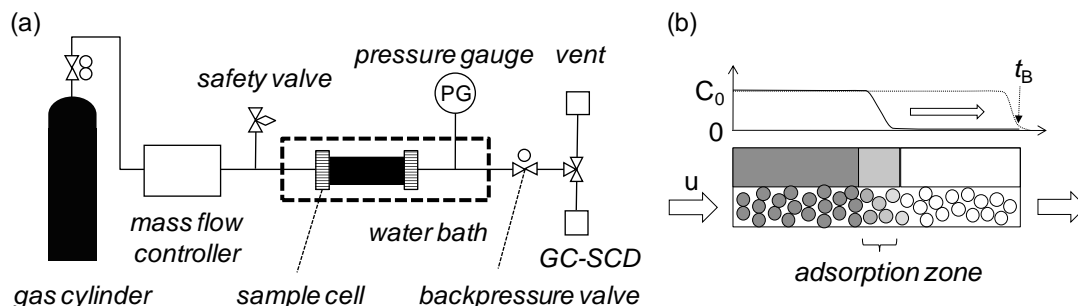
Figure 2: (a) Experimental setup for the measurement of a breakthrough curve under different pressure and temperature, (b) schematic diagram of breakthrough in a packed-bed.

packed in a glass column and were outgassed at 473 K for 2 h in a nitrogen gas flow before the measurement. The temperature and pressure inside the sample cell were varied in the ranges of 311-331 K and 0.1-0.9 MPa, respectively. The pressure inside the sample cell was controlled using a backpressure valve, while the temperature of the sample cell was controlled using a water bath. During the measurement of BTC, model gas with the initial concentration of HS (C_0 = 200 mol.ppm) was continuously introduced to the sample cell using a mass flow controller. The other chemical species contained in the model gas and the concentrations were hydrogen: 50 mol.%, carbon dioxide: 15 mol.%, ethylene: 25 mol.% and propylene: 10 mol.%, respectively. Then, the transient change in the outlet concentration of HS (C) was measured using a gas chromatograph (GC) equipped with a photomultiplier detector. As a result, a breakthrough curve was obtained from the relation between time and the concentration of HS in the gas sampled at the exit of the packed bed as illustrated in Figure 2(b). The breakthrough time was defined as the time at which the ratio (C/C_0) between the concentration of HS at the exit of the packed bed and the initial HS concentration was equal to 0.05. We estimated the total amount, Q, of HS adsorbed on the packed-bed at the breakthrough time according to the following Eq. 1.

$$Q = \frac{c_0 F M_A t_b}{V w} \tag{1}$$

Here c_0, F, M_A, t_b, V and w were the initial HS concentration, the gas flow rate, the molecular weight of HS, the breakthrough time, the molar volume of mixed gas at the measured temperature and the weight of the bed, respectively. The desulfurized gas was also analyzed using a sulfur chemiluminescence detector (GC-SCD, Shimadzu 2010 – Antek 7090 model.) The detection limit of the GC-SCD was 10 ppb.

3. Results and discussion

3.1 Porous properties of the adsorbent

Figure 3(a) shows the adsorption and desorption isotherms of N_2 on PIO. The BET specific surface area of PIO is 120 m^2/g, because of the presence of the micropores and mesopores which act as the adsorption sites of HS. It is found that PIO possesses the broad pore size distribution because of the presence of the macropores. To consider the intra-particle mass transfer, we estimate the effective pore diffusivity, D_{eff}, according to the Eq. 2, which gives the pore diffusivity in the transitional region between the Knudsen diffusion and molecular diffusion.

$$\frac{1}{D_{eff}} = \frac{1}{D_{AB}} + \frac{1}{D_K} \tag{2}$$

Here D_{AB} and D_K are the molecular diffusivity and the Knudsen diffusivity as expressed by the Eqs. 3 and 4.
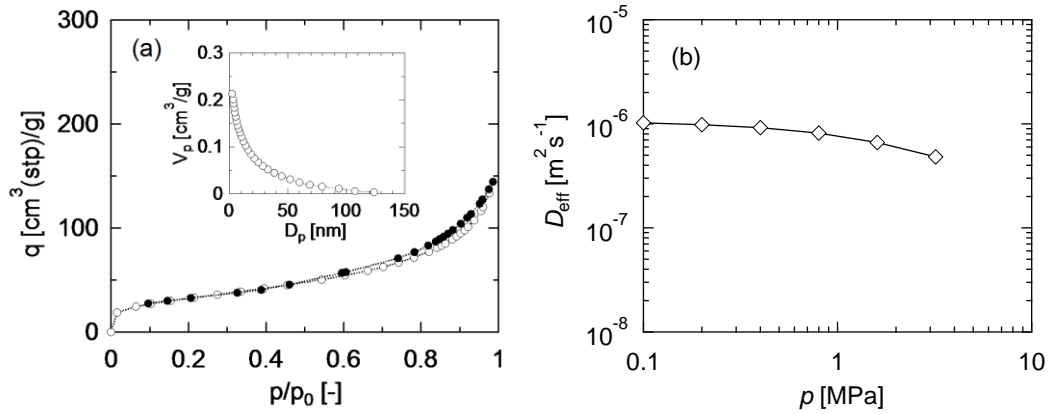
Figure 3: (a) Adsorption and desorption isotherms of nitrogen and pore size distribution of PIO, (b) effective pore diffusivity of a HS molecule in PIO particle.
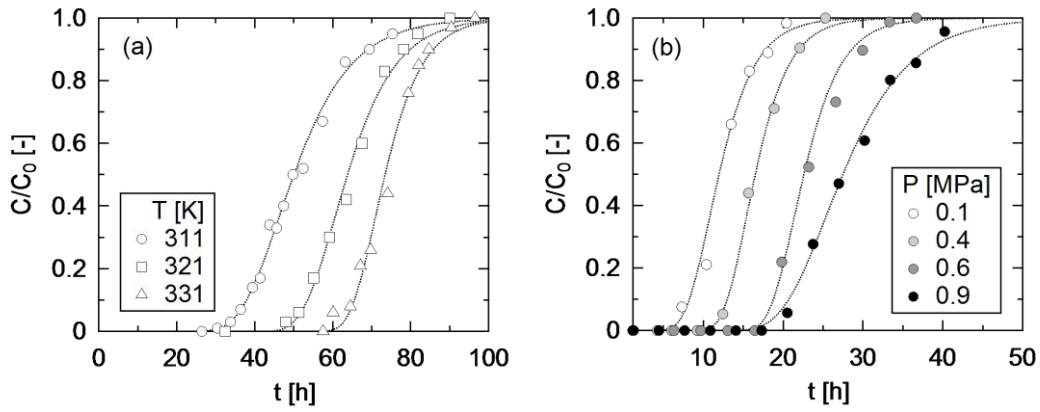

Figure 4: (a) BTCs measured under different temperature (P=0.1 MPa, GHSV=1600), (b) BTCs measured under different pressure (T=311 K, GHSV=4000).

$$D_{AB} = \frac{4.58 \times 10^{-10} T^{1.75} \left(1/M_A + 1/M_B\right)^{1/2}}{p \left[\left(\sum v\right)_A^{1/3} + \left(\sum v\right)_B^{1/3}\right]^2} \tag{3}$$

$$D_K = 1.53 \times 10^{-9} d_{p,mean} \sqrt{\frac{T}{M_A}} \tag{4}$$

where T, M, p, Σv and $d_{p,mean}$ are temperature, molecular weight, pressure, molar volume and the mean pore diameter of the adsorbent, respectively. The subscripts "A" and "B" represent HS and propylene, respectively. $d_{p,mean}$ can be determined as 7.2 nm from the isotherms of nitrogen. Figure 3(b) shows the effect of pressure on the effective pore diffusivity of a HS molecule. Although the effective pore diffusivity gradually decreases with the increase in pressure, we can expect the rapid mass transfer of HS inside the PIO particles even under the condition of high pressure.

3.2 Adsorption performance of the adsorbent
Figure 4(a) shows the BTCs measured at different temperature. For example, one can see that the breakthrough time of the curve measured at 311 K is approximately 35 h. It is noteworthy that the
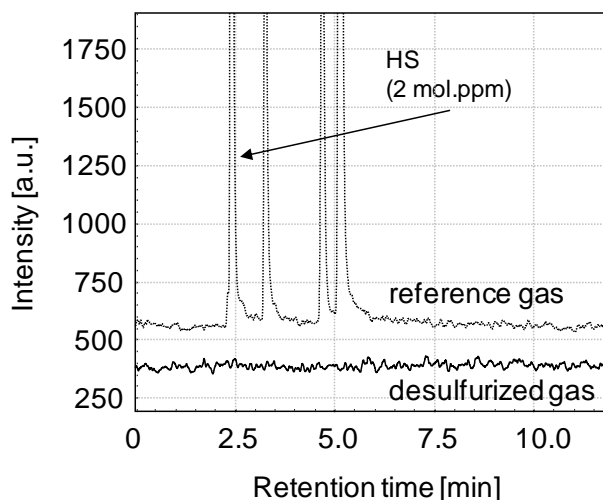
1198

Figure 5: An example of GC-SCD chromatogram of the desulfurized gas.

breakthrough time, in other words, the capacity of PIO for adsorbing HS, increases with the increase in the temperature. This shows that HS molecules are removed by the chemical reaction with iron oxide contained in limonite, even at the temperature lower than 400 K. Although the detail of the reaction mechanism has not yet been clarified, it is assumed that iron oxide changes to iron sufides, such as pyrite (FeS_2) and pyrrhotite ($Fe_{1-x}S$), by the sulfidation reaction with HS. On the other hand, the BTCs measured under the condition of different pressure are shown in Figure 4(b). The breakthrough time also increases with the increase in the pressure. This is probably because the sulfidation reaction can be enhanced under the higher pressure.

In the process shown in Figure 1(c), the possible operating conditions of the desulfurization unit are 311 K and 0.9 MPa. Under the conditions, we have estimated that the amount of HS adsorbed on PIO is as much as 4.1×10^{-3} g/g-adsorbent at the breakthrough time. Figure 5 shows the chromatograms obtained by measuring the standard gas and the desulfurized gas which is sampled before the breakthrough time, respectively. In the chromatogram of the standard gas, we can observe the large peak corresponding to HS at the retention time of 2.5 min. On the other hand, since we cannot observe the peak of HS in the chromatogram of the desulfurized gas, the concentration of HS is less than the detection limit (10 ppb) of GC-SCD. Thus, we have confirmed the adsorption performance of PIO as the adsorbent for HS at low temperature.

4. Conclusions

In the development of the process to produce polymer-grade propylene from crude bioethanol which contained the sulfur impurities, we examined adsorption desulfurization to remove hydrogen sulfide (HS), which was derived from the sulphur impurities contained in bioethanol, employing porous iron oxide (PIO) as an adsorbent. We found that PIO possessed a broad pore size distribution as well as a large specific surface area, which were suitable for adsorption of HS efficiently. The performance of PIO was evaluated by the measurement of a packed-bed breakthrough curve in a gaseous phase under the conditions of varied temperature and pressure. As a result, we confirmed that the concentration of HS in the desulfurized gas could be reduced lower than 10 ppb, which was the desired sulfur concentration as polymer-grade propylene. In our subsequent study, we will examine the details of the reaction mechanism between PIO and HS at low temperature.

Acknowledgement

References

Chaichanawong J., Yamamoto T., Ohmori T., Endo A., 2010, Adsorptive desulfurization of bioethanol using activated carbon loaded with zinc oxide, Chemical Engineering Journal, 165, 218-224, DOI: 10.1016/j.cej.2010.09.020.

Furumoto Y., Harada Y., Tsunoji N., Takahashi A., Fujitani T., Ide Y., Sadakane M., Sano T., 2011, Effect of acidity of ZSM-5 zeolite on conversion of ethanol to propylene, Applied Catalysis A: General, 399, 262-267, DOI: 10.1016/J.APCATA.2011.04.009.

Goto D., Harada Y., Furumoto Y., Takahashi A., Fujitani T., Oumi Y., Sadakane M., Sano T., 2010, Conversion of ethanol to propylene over HZSM-5 type zeolites containing alkaline earth metals, Applied Catalysis A: General, 383, 89-95, DOI: 10.1016/J.APCATA.2010.05.032.

Inoue K., Inaba M., Takahara I., Murata K., 2010, Conversion of ethanol to propylene by H-ZSM-5 with Si/Al(2) ratio of 280, Catalysis Letters, 136, 14-19, DOI: 10.1007/s10562-010-0315-2.

Kravanja P., Friedl A., 2010, Evaluation of ethanol from lignocellulosic biomass - process scenarios for Austria, Chemical Engineering Transactions, 21, 1141-1146, DOI: 10.3303/CET 1021191.

Landaud S., Helinck S., Bonnarme P., 2008, Formation of volatile sulfur compounds and metabolism of methionine and other sulfur compounds in fermented food, Applied Microbiology and Biotechnology, 77, 1191-1205, DOI: 10.1007/s00253-007-1288-y.

Muroi T., 2003, Industrial Noble Metal Catalyst. JETI, Tokyo, Japan (in Japanese)

Porzio G.F., Prussi M., Chiaramonti D., 2011, Process analysis and modelling for 2nd generation lignocellulosic bioethanol production, Chemical Engineering Transactions, 25, 869-874, DOI: 10.3303/CET1125145.

Song Z.X., Takahashi A., Mimura N., Fujitani T., 2009, Production of propylene from ethanol over ZSM-5 zeolites, Catalysis Letters, 131, 364-369, DOI: 10.1007/s10562-009-0071-3.